Journal of the European Ceramic Society **12** (1993) 413–420

Preparation, Microstructure and Properties of $MgSiN_2$ Ceramics

W. A. Groen, M. J. Kraan & G. de With*

Philips Research Laboratories, PO Box 80000, 5600 JA, Eindhoven, The Netherlands

(Received 10 February 1993; revised version received 19 April 1993; accepted 1 June 1993)

Abstract

The synthesis of $MgSiN_2$ powder, starting from the metal nitrides, is described. The powder is resistant against oxidation in air up to 800°C. From the prepared powder full dense $MgSiN_2$ ceramics can be sintered at 1550°C. The samples were sintered in a closed Mo vessel to prevent evaporation of magnesium nitride. Phase composition, chemical properties and the mechanical properties of the as-prepared ceramics are described. The ceramics are oxidation resistant in air at least up to 920°C. The thermal conductivity at room temperature is estimated at 17 W/m K. A reasonable strength of 270 MPa and a rather good fracture toughness of about 4·3 MPa $m^{1/2}$ are obtained. A hardness of about 15 GPa and a Young's modulus of 235 GPa have been measured. Considerable improvement in properties is expected when the processing conditions, well within reach, are optimised.

Die Synthese von $MgSiN_2$-Pulver, ausgehend von Metallnitriden, wird beschrieben. Das Pulver ist gegen Oxidation in Luft bis zu 800°C beständig. Aus dem Pulver können dichte $MgSiN_2$-Keramiken bei 1500°C gesintert werden. Die Proben wurden in einem geschlossenen Mo-Gefäß gesintert, um das Abdampfen von Magnesiumnitrid zu verhindern. Die Phasenzusammensetzung, die chemischen Eigenschaften und die mechanischen Eigenschaften der unbehandelten Keramiken werden beschrieben. Die Keramiken sind in Luft mindestens bis 920°C oxidationsbeständig. Die thermische Leifähigkeit bei Raumtemperatur beträgt etwa 17 W/m K. Es wurde eine mäßige Festigkeit von 270 MPa und eine ziemlich gute Bruchzähigkeit von 4·3 MPa $m^{1/2}$ erzielt. Die Härte ergab einen Wert von 15 GPa und der Elastizitätmodul betrug 235 GPa. Eine erhebliche Verbesserung der Eigenschaften wird erwartet, wenn, was in naher Zukunft möglich ist, die Prozeßbedingungen optimiert werden.

Les auteurs décrivent la synthèse d'une poudre de $MgSiN_2$, à partir de nitrures métalliques. La poudre résiste à l'oxydation dans l'air jusqu'à 800°C. A partir de cette poudre, on peut fritter, à 1550°C, des céramiques denses en $MgSiN_2$. Les échantillons ont été frittés dans un récipient en Mo fermé pour éviter l'évaporation du nitrure de magnésium. La composition des phases, les propriétés chimiques et mécaniques des céramiques préparées de cette façon sont décrites. Le céramiques résistent à l'oxydation dans l'air au moins jusqu'à 920°C. La conductivité thermique à température ambiante a été estimée à 17 W/m K. Un module de rupture raisonnable de 270 MPa et une ténacité plutôt bonne de 4·3 MPa $m^{1/2}$ ont été obtenus. Une dureté d'environ 156 GPa et un module de Young de 235 GPa ont été mesurés. Une amélioration considérable des propriétés est attendue lorsque les conditions d'élaboration auront été optimisées.

1 Introduction

Aluminium nitride ceramics are of interest because they combine a high thermal conductivity with a high electrical resistance at room temperature. As discussed by Slack[1] only a few materials are known with a high electrical resistance at room temperature for which the thermal conductivity at ambient temperatures exceeds 1 W/cm K. Most of them crystallise in a diamond-like structure, e.g. BeO and AlN. In all of these structures the atoms are tetrahedrally coordinated. Unlike metals, in these compounds the heat flow is primarily carried by phonons. As a result the thermal conductivity of these materials is strongly dependent on impurities, which is due to phonon scattering.

$MgSiN_2$ is noted as an alternative ternary compound[1] with a high thermal conductivity. The

* Also affiliated with the Centre for Technical Ceramics, Eindhoven University of Technology, PO Box 513, 5600 MD, Eindhoven, The Netherlands.

Journal of the European Ceramic Society 0955-2219/93/$6.00

preparation of the ternary nitride $MgSiN_2$ has first been reported by David and Lang.[2] Using either Mg_2Si or a mixture of the binary nitrides Mg_3N_2–Si_3N_4, they observed the appearance of a new phase by X-ray diffraction after heating the starting powders in nitrogen to 1200°C. It was concluded that this phase has a composition which is approximately $MgSiN_2$. The structure of $MgSiN_2$ has been found to be isotypical to $BeSiN_2$.[3–5] The compound crystallises in an orthohombic structure (spacegroup $Pna2_1$, no. 33), which is derived from the Wurtzite structure. The hexagonal structure is distorted because of the presence of two metal atoms and displacement of the nitrogen atoms from their ideal positions in the Wurtzite structure. ^{15}N-NMR experiments on enriched ^{15}N samples indicated a complete ordering of the Mg and Si atoms.[6] The band gap is reported to be 4·8 eV as calculated from diffuse reflectance spectra.[7]

This paper describes the preparation of $MgSiN_2$ powder and ceramics starting from the binary nitrides. The phase composition, thermal stability, microstructure and mechanical properties of the as-prepared ceramics are reported.

2 Experimental

The synthesis of the $MgSiN_2$ powder was done starting from Mg_3N_2 (Cerac, 99·9%) and amorphous Si_3N_4 (Sylvania, SN402). A stoichiometric mixture of the powders was mixed in an agate mortar. The mixture was loaded in an alumina crucible which was placed in a stainless-steel tube. The stainless-steel tube was sealed mechanically to prevent evaporation of Mg_3N_2. The tube was subsequently heated in a nitrogen flow for 16 h at 1250°C. To minimise oxygen contamination the handling of the starting materials was performed in an argon atmosphere. After firing, the resulting powder was milled using an agate ball-mill in hexane for 24 h. The particle size distribution of the as-prepared and of the milled powder was measured with a Shimadzu SA-CP4 centrifugal particle size analyser.

From the resulting powder mixture pellets were prepared applying two methods. Using the first method (samples #1) pellets were pressed (diameter ≈ 30 mm, thickness ≈ 4–6 mm) using a polymethyl methacrylate (PMMA) die at 5 MPa. These pellets were subsequently cold isostatically repressed at 200 MPa. The resulting density of the green compacts is ≈ 50%.

Using the second method (samples #2), 25 g $MgSiN_2$ powder was dispersed in 200 ml ethanol with 200 mg *para*-hydroxy benzoic acid. The dispersion was filtrated over a 0·2 μm filter (diameter 30 mm) with a pressure of 1 bar (1 bar = 10^5 Pa). The resulting pellets were dried at 150°C at a pressure of 10 mbar for 2 h. This yielded green compacts of approximately 50% density.

The pellets were placed in a molybdenum vessel which was closed using arc welding in an argon ambient at 200 mbar pressure. The pellets were buried in a powder bed of $MgSiN_2$ powder. In the case where no powder bed was used, the sintered pellets show bubbles inside which are probably due to evaporation of Mg during sintering. The vessel was heated in hydrogen/nitrogen ambient (5% H_2) in a horizontal tube furnace. The heating rate was 1000°C/h to the set point of 1550°C. The sample was kept at this temperature for 5 h and was cooled down to room temperature with a rate of 200°C/h.

Phase identification was carried out using X-ray diffraction (XRD) (Philips PW1800 diffractometer) using monochromatized CuKα radiation. For elemental analysis a ceramic sample was dissolved in a Na_2CO_3 melt. Magnesium and silicon were analysed using inductive coupled plasma emission spectroscopy (ICP) after dissolving the melt in diluted HCl. The oxygen and nitrogen content was measured using a Leco TC 436 O_2/N_2 analyser.

The thermal stability against oxidation of the ceramic sample was studied using thermogravimetric analyses (TGA) with a Perkin Elmer PC-TGA7 at temperatures up to 920°C in air. Differential thermal analysis (DTA) was performed to investigate phase transformations and the thermal stability of the powder. DTA measurements were performed using a home-build apparatus with a two thermocouple configuration. TGA and DTA measurements were made in dry flowing air at ambient pressures.

The density, d, of the samples was determined by Archimedes method. The longitudinal wave velocity, v_l, and the shear wave velocity, v_s, were measured at 10 and 20 MHz, respectively, using the pulse-echo method. From d, v_l and v_s, Young's modulus, E, and Poisson's ratio, ν, were calculated with the usual formulae for isotropic materials. No correction for damping was applied since the loss tangent was less than 0·05.[8] The standard deviation in Young's modulus was estimated to be about 2 GPa.

The Vickers hardness, H_v, was measured on a polished specimen. A load of 20 N was applied for about 15 s. The average standard deviation using five readings was about 1·6 GPa.

The fracture toughness, K_{Ic}, was measured in a dry N_2 gas atmosphere (≈ 200 ppmV H_2O) with the three-point bend test (span 12 mm, crosshead speed 10 mm/min), using specimen of size 1 × 3 × 15 mm^3. A notch with a relative depth of about 0·15 and a width of 100 μm was sawn in the specimen. Pre-

cracking was done by a Knoop indentation (10 N load) at the notch root on both sides of the specimen. The compliance factor was calculated as described in Ref. 9. The small type of specimen makes efficient use of the available material while retaining reliability and accuracy.[10] Normally, five specimens were used for each K_{1c} determination resulting in an average sample standard deviation of 0·2 MPa $m^{1/2}$. The strength was measured in the same bending set-up. Samples were sawn with 100 μm diamond wheel. Usually, five specimens were used resulting in a sample standard deviation of 30 MPa.

Thermal diffusivity measurements were made using a photo flash method, which is described in detail by Söllter *et al.*[11] The thermal expansion coefficient was determined in N_2 in the temperature range from 20 to 600°C using a specimen of 1 cm length in a dual rod dilatometer (Netsch). For reference a fused silica sample was used with an expansion coefficient of $0{\cdot}55 \times 10^{-6}$ K.

3 Results

The reacted powder has a white colour, contrary to the violet and dark-grey colours as reported in the literature.[3] XRD indicated that the powder is nearly single phase $MgSiN_2$.[12] The other phases which were observed are MgO (Ref. 13) and α-Si_3N_4 (Ref. 14). Probably, some amorphous SiO_2 is also present. The total amount of other phases is below 5%, due to oxygen contamination in the amorphous Si_3N_4 precursor.

The unit cell parameters are presented in Table 1. For comparison, the unit cell data as reported in the literature are also given.[2,5,12,15] The results of the analysis of the oxygen and nitrogen content are presented in Table 2.

To investigate the phase width of the composition Mg:Si = 1:1, samples with 5 mol% excess of $MgN_{2/3}$ and 5 mol% excess of $SiN_{4/3}$ were prepared and examined with XRD. In case of excess Si_3N_4, α-Si_3N_4 was found while in case of excess Mg_3N_2, MgO was found. The XRD patterns for both compositions were indistinguishable (apart from the other phases) from the composition 1:1 indicating similar unit cell parameters and consequently a limited phase width.

Table 1. Unit cell parameters of $MgSiN_2$ powder and ceramics, literature data are included

Sample	*a (nm)*	*b (nm)*	*c (nm)*	*V* ($\times 10^{-30}$ m^3)
David *et al.*[2,12]	0·5279	0·6476	0·4992	171
Zykov[11]	0·5272	0·6482	0·4980	170·18
Wild *et al.*[5]	0·5275	0·6455	0·4978	169·5
Powder	0·5282	0·6474	0·4991	170·64
Ceramic	0·5266	0·6472	0·4983	169·83

Table 2. Compositions of the powder and ceramics

Element	*Powder (wt%)*	*Ceramic sample (wt%)*
Mg	—	30·1 (1·5)
Si	—	33·6 (1·5)
N	30·7 (1·5)	30·7 (1·5)
O	3·7 (0·2)	3·7 (0·2)

Particle size analyses of the powder dispersed in ethanol showed the existence of relatively large particles (> 4 μm). Therefore, the powder was milled for 24 h in hexane to obtain a narrower range in the particle size distribution. The particle size distributions before and after milling are presented in Fig. 1. Scanning electron microscopy (SEM) micrographs of the prepared powder showing agglomerates of $MgSiN_2$ particles are shown in Fig. 2.

After sintering in the Mo vessel the pellets show a light grey colour. The density of the pellets is 3·11 g/cm^3. The density as calculated from the crystal structure is 3·128 g/cm^3, indicating that nearly a full density has been achieved. The XRD pattern is presented in Fig. 3. The measured lattice constants are given in Table 1. Other phases

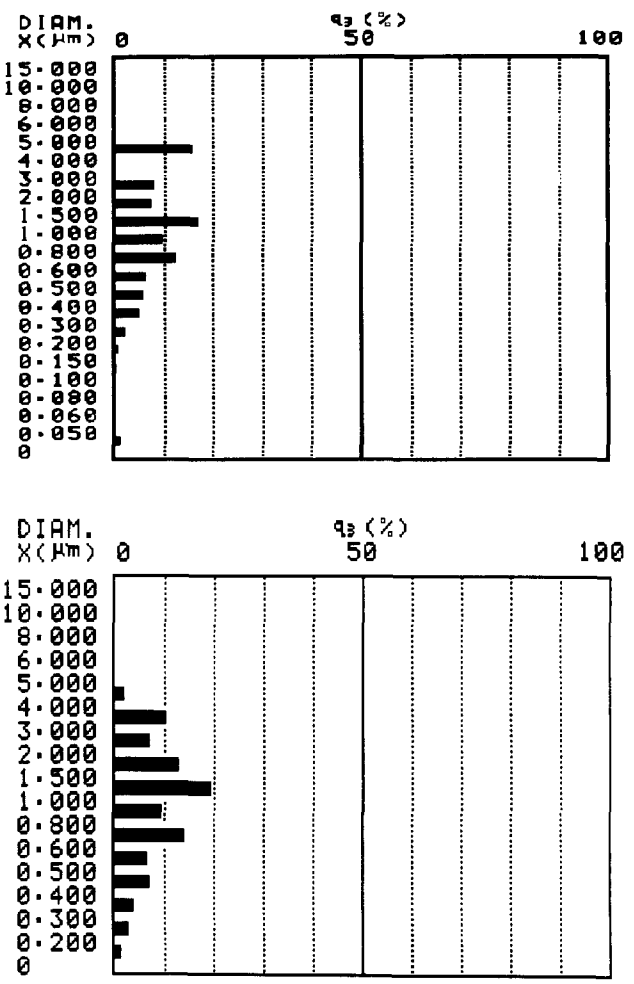

Fig. 1. The particle size distribution of the $MgSiN_2$ powder before and after 24 h milling in hexane. The median diameters are 1·02 μm and 0·94 μm and the modal diameters are 1·21 μm and 1·21 μm, respectively, before and after milling.

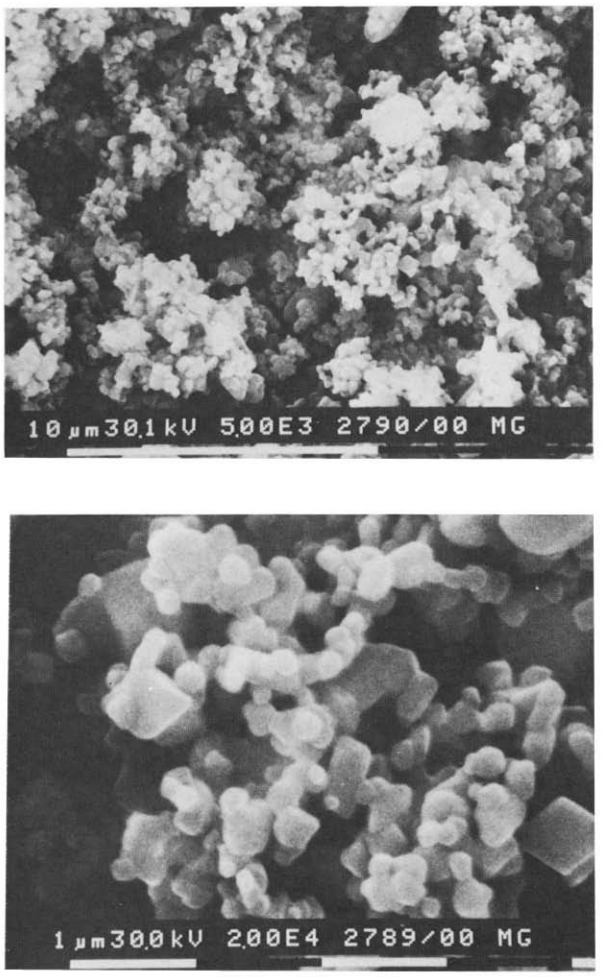

Fig. 2. SEM micrograph at two magnifications of the unmilled, as-prepared powder showing agglomerates of $MgSiN_2$ particles.

observed in the sample are Mg_2SiO_4 (Ref. 16) and of β-Si_3N_4 (Ref. 17). The estimated amount of both is less than 5%. The results of the elemental analysis of a ceramic sample are shown in Table 2. The overall composition of the sample, including second phases, is calculated as $Mg_{1.00}Si_{0.97}N_{1.77}O_{0.19}$. From this result it can be estimated, assuming all oxygen present in Mg_2SiO_4, that the sample contains approximately 5% Mg_2SiO_4 and 0·7% Si_3N_4 as other phases.

The grain sizes and the morphology of the second phases of the sintered samples has been examined using an SEM. In Fig. 4 SEM micrographs are shown of a fractured sintered sample at different magnifications. The micrographs indicate that nearly full density has been achieved but also show a substantial amount of second phases.

In order to obtain more detailed information about the microstructure, some of the pellets were polished and etched using a saturated KOH solution in water, a 60% H_3PO_4 solution or a 10% HF solution. All methods failed in achieving a well-etched surface. The pellet which has been placed for 16 h in the KOH solution showed no reaction at all, indicating a good chemical resistance of the material towards alkaline solutions. The pellets that were placed in the acid solutions (for various times and temperatures) showed a very non-uniform etching. SEM micrographs of the sample which was etched for 20 s in a 1% HF solution in water are shown in Fig. 5.

DTA measurements performed on powder showed no signal at temperatures up to 800°C. This demonstrates that no phase transitions in the crystal structure occur. Starting from 800°C a large signal is observed which originates from oxidation of the sample. Mg_2SiO_4 and a broad peak, which probably corresponds to amorphous SiO_2, were observed with XRD for a powder sample which was heated at 1000°C in air. TGA measurements on the ceramics showed no gain in weight up to 920°C.

Measurements of the thermal diffusivity (meas-

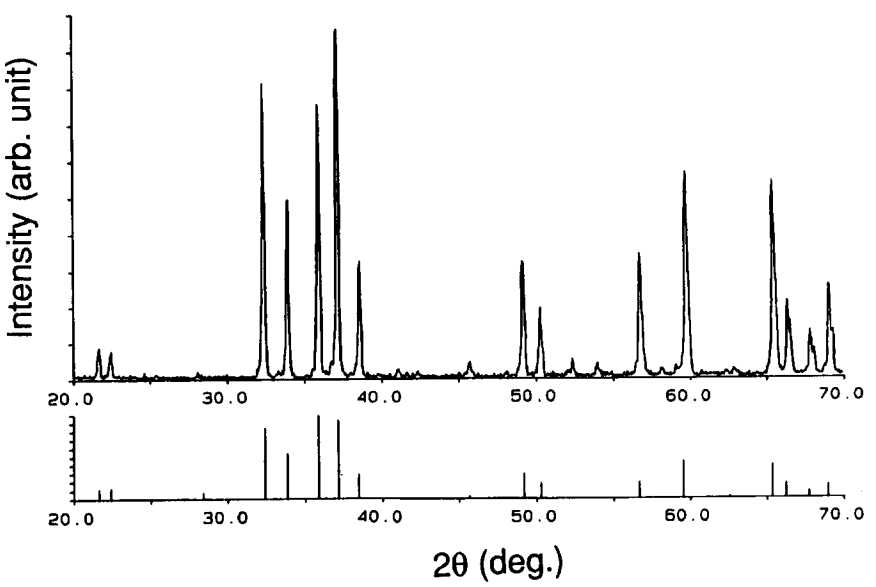

Fig. 3. The XRD pattern of the ceramic $MgSiN_2$ sample. For comparison the pattern according to Ref. 12 is presented below the observed pattern.

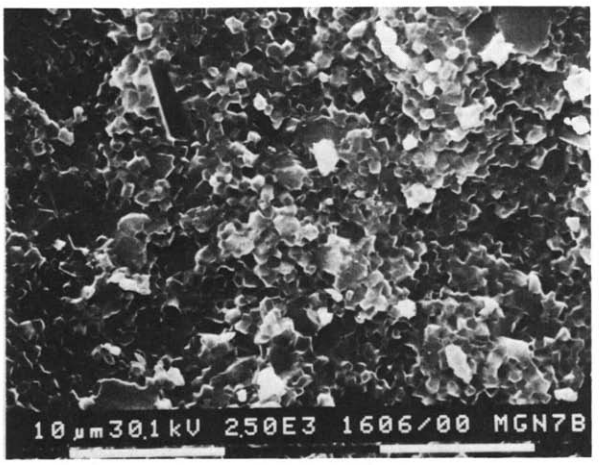

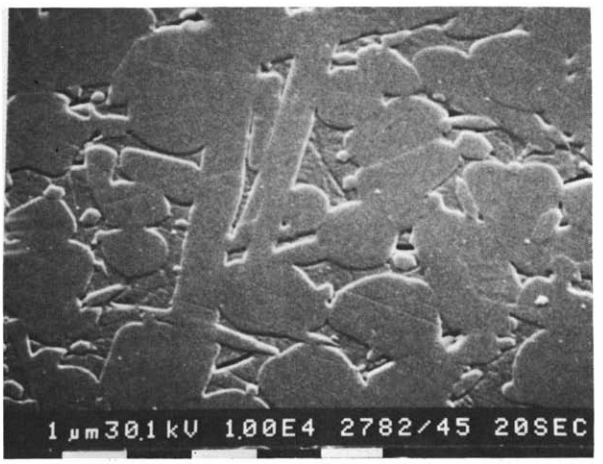

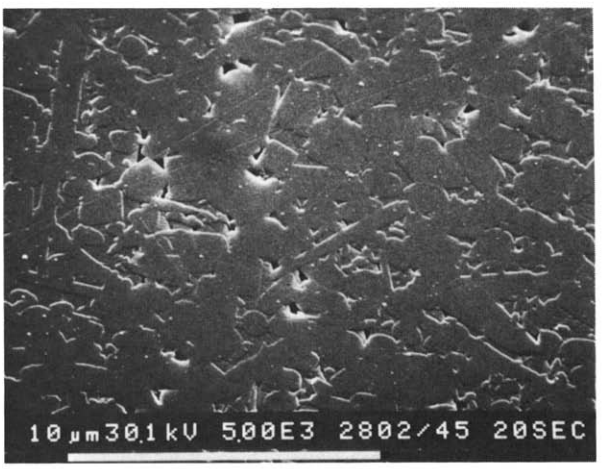

Fig. 4. SEM micrographs at two magnifications of a fracture surface of the sintered ceramic $MgSiN_2$ sample.

Fig. 5. SEM micrographs of a $MgSiN_2$ ceramic sample which has been etched for 20 s in an aqueous solution of 1% HF.

ured at Hoechst A.G.), l, resulted in a value of 0·0738 cm^2/s. From this value the thermal conductivity, k, can be estimated according to

$$k = ldC_p$$

Using the known C_p value of AlN (Ref. 18) of 738 J/kg K and the density, d, of 3·11 g/cm^3, the thermal conductivity is calculated to be 17 W/m K.

The results for the measurements of the hardness, H_v, the fracture toughness, K_{Ic}, and the strength, σ, on four different samples are presented in Table 3. For comparison the reported mechanical properties of Al_2O_3, γ-aluminium oxynitride (Alon, see, for example, Ref. 20) and AlN are also presented.[19–22] The elastic properties of sample #2·2 (see Table 3) are presented in Table 4. Again, literature data for Al_2O_3, Alon and AlN are also included.[19,20,23]

The relative dielectric constant, ε_r, has been measured on a ceramic sample from batch #2 (thickness 1·27 mm, diameter 18 mm) at room temperature using a HP4275A LCR meter. On both sides of the sample a thin ($\approx$ 250 nm) silver layer was deposited by sputtering. The measurements were performed between 10 kHz and 10 MHz. The value

Table 3. Mechanical properties of $MgSiN_2$ ceramics of four samples[a]

Sample	H_v (*GPa*)	K_{Ic} ($MPa\,m^{1/2}$)	σ (*MPa*)
$MgSiN_2$ #1·1	15·9 (1·6, 5)	3·14 (0·24, 5)	231 (28, 6)
$MgSiN_2$ #1·2	15·3 (0·8, 5)	3·17 (0·22, 5)	249 (21, 7)
$MgSiN_2$ #2·1	15·2 (1·6, 5)	4·33 (0·53, 5)	266 (9, 5)
$MgSiN_2$ #2·2	14·2 (0·5, 5)	4·363 (0·61, 4)	276 (35, 4)
Al_2O_3	19·5 (Ref. 19)	4·5 (Ref. 19)	450 (Ref. 21)
Alon	19 (Ref. 20)	2·4 (Ref. 20)	300 (Ref. 20)
AlN	12 (Ref. 21)	2·7 (Ref. 22)	340 (Ref. 21)

[a] Standard deviation and the number of measurements used are given in parentheses. For comparison the properties for Al_2O_3, Alon and AlN are also presented.

Table 4. Elastic properties of $MgSiN_2$ ceramics (sample #2·2 of Table 3)[a]

Sample	*E (GPa)*	*ν*
$MgSiN_2$	235	0·232
Al_2O_3	398 (Ref. 19)	0·235 (Ref. 19)
Alon	330 (Ref. 20)	0·253 (Ref. 20)
AlN	315 (Ref. 23)	0·245 (Ref. 23)

[a] For comparison the properties for Al_2O_3, Alon and AlN are also presented.

for the relative dielectric constant was measured to be 10·5. This value is close to the value of AlN (Ref. 24) which is 9·1.

The thermal expansion of a $MgSiN_2$ sample, #2·1, as a function of temperature was measured in N_2. The thermal expansion coefficient, α, over the temperature range from 20 to 600°C was measured to be $5{\cdot}8 \times 10^{-6}$/K.

4 Discussion

$MgSiN_2$ is a covalent compound, and hence limited atomic mobility is hampering densification at acceptable temperatures. However, it is shown that $MgSiN_2$ can be sintered to full density at a temperature of 1550°C suggesting that a liquid phase is present, enhancing sintering. This liquid phase is most probably formed in the system MgO–SiO_2 (Ref. 25) between approximately 40 and 60 mol% MgO at a temperature above ≈1550°C.

Wet chemical etching experiments showed that the $MgSiN_2$ ceramics are stable in a KOH solution. This result was unexpected since AlN can be dissolved (slowly) in alkaline solutions.

The as-prepared powder is stable in air at temperatures up to 800°C. The TGA measurements indicate that the ceramic sample is stable in air to temperatures up to 920°C. The greater stability of the ceramic sample with respect to the powder is due to the reduced surface area and probably to the formation of a thin protective layer consisting of SiO_2 or Si_2N_2O on the surface.

The value for the thermal conductivity, k, of 17 W/m K is a promising value for a ceramic material which is electrically insulating at high frequencies. Higher values are only obtained for AlN, BeO, Alon, high-purity MgO and high-purity Al_2O_3. Because of the presence of second phases as well as the oxygen contamination, it is expected that the thermal conductivity can be increased considerably by careful powder preparation and processing and using better quality precursor materials. In particular when one considers that the present results for this compound are the first ones while the materials have been optimised to a great deal. However, the superlattice present in $MgSiN_2$ automatically lowers the thermal conductivity as compared to AlN.

Many papers have been published in which the influence of the microstructure on the thermal conductivity of AlN is described. Oxygen is a major impurity in AlN resulting in the formation of aluminium vacancies in the AlN lattice. This reduces the thermal conductivity of single crystals[26] and ceramics[27] drastically. Second phases, due to the presence of sintering additives during liquid phase sintering of AlN ceramics, cover the AlN grains by a second phase oxide, contributing also to a poor thermal conductivity in ceramics. An arrangement of the second phases in triple points increases the thermal conductivity. Values above 150 W/m K are only obtainable if the amount of impurities in the AlN lattice, the distribution and amount of the second phase at the grain boundaries and the gradient of oxygen and sintering additives at the grain boundaries are optimised.[28]

Comparable to AlN, for $MgSiN_2$ it is very probable that incorporation of oxygen in the lattice also results in a drastic decrease of the thermal conductivity. The introduction of oxygen can be described by the following reactions, using the notation of Kröger and Vink:[29]

$$2MgSiO_3 \leftrightharpoons 2Mg^{*}_{Mg} + 2Si^{*}_{Si} + 6O^{\cdot}_{N} + V''_{Mg} + V''''_{Si} \quad (1)$$

However, in $MgSiN_2$ it should be possible to decrease the cationic vacancy concentrations by balancing the Mg to Si ratio. This can be best visualised by the incorporation of MgO in the lattice:

$$2MgO \leftrightharpoons Mg^{*}_{Mg} + 2O^{\cdot}_{N} + Mg''_{Si} \quad (2)$$

In this case charge compensation is achieved by the Mg''_{Si} defect and no cationic vacancies are formed. A strong dependence of the thermal conductivity on the oxygen content may possibly be cancelled in this way. The addition of MgO in the lattice is limited in view of the fact that XRD showed $MgSiN_2$ to be a compound with a narrow phase width (line compound). The solubility is probably sufficient though for an effective cancelling of the cationic vacancies.

SEM images of the microstructure of an etched surface of the sintered ceramic $MgSiN_2$ sample as shown in Fig. 4, indicate that the thermal contact between the grains may sometimes be poor. Therefore, a reduction of the grain boundary phases will improve the thermal conductivity. Also sintering additives which result in segregation of the second phases at triple points between the grains will improve the thermal conductivity.

The hardness of the various samples is approximately constant at about 15 GPa. This value is somewhat lower than for Al_2O_3 and Alon but higher

Table 5. Characteristic parameters, R and R', for the thermal shock resistance of $MgSiN_2$ ceramics[a]

	$MgSiN_2$	Al_2O_3	*Alon*	*AlN*
σ (MPa)	240–270[b]	450 (Ref. 21)	300 (Ref. 20)	340 (Ref. 21)
E (GPa)	235	398 (Ref. 19)	330 (Ref. 20)	315 (Ref. 23)
ν	0·232	0·235 (Ref. 19)	0·253 (Ref. 20)	0·245 (Ref. 23)
α (10^{-6}/K)[c]	5·8	7·9 (Ref. 30)	7·8 (Ref. 30)	4·8 (Ref. 30)
k (W/m K)	17	20 (Ref. 19)	30 (Ref. 20)	150 (Ref. 29)
R (K)	130–150	110	90	170
R' (kW/m)	2·2–2·5	2·2	2·6	2·5

[a] For comparison the data for Al_2O_3, Alon and AlN are also presented.
[b] Values from Table 3.
[c] As measured between 20 and 600 C.

than for AlN. The value for Young's modulus is, on the other hand, lower than for Al_2O_3 or Alon or AlN. Even when corrected for porosity in some way, the value for E remains low. The fracture toughness of samples #2·1 and #2·2 is significantly higher than for samples #1·1 and #1·2. This is the result of improved processing. The increase in toughness, a factor of about 1·4, is only partially reflected in the strength. Here an increase of a factor about 1·1 is obtained. This difference is probably related to the differences in grain size. A further increase of about 30% should be thus realisable.

The thermal shock resistance of ceramics can be conveniently characterised by the following parameters:

$$R = \sigma(1 - \nu)/E\alpha \tag{3}$$

$$R' = kR \tag{4}$$

where the symbols have the meaning as defined earlier. The parameter R characterises the materials resistance towards thermal shock for high heat transfer conditions. The parameter R' does the same but for mild heat transfer conditions. From the experimental data the parameters R and R' are calculated and given in Table 5. For comparison the values as calculated for AlN, Alon and Al_2O_3 are also indicated. From Table 5 it can be concluded that the thermal shock resistance of $MgSiN_2$ is better than for Al_2O_3 and Alon, and about nearly as good as for AlN. By improving the processing it is expected that an increase in strength of at least 30% can be realised (see before). As a guess, an improvement in the thermal conductivity of at least a factor of 2 should be achievable. This would improve the R and R' parameter by a factor 1·3 and 2·6, respectively, making the material comparable to SiC and reaction bonded silicon nitride with respect to R. This improvement would not rank the R' parameter as good as for SiC and AlN but considerable better than for most other ceramics.

An investigation of the high-temperature electrical properties of $MgSiN_2$ ceramics will be presented in a forthcoming paper. Also a more detailed investigation about the stability at high temperatures of the as-prepared ceramics is planned.

Acknowledgements

Grateful acknowledgements are due to J. Timmers for the X-ray analysis, to C. J. Geenen for the SEM work, to A. C. A. Jonkers for the elemental analyses, to N. A. M. Sweegers for the measurements regarding the mechanical properties and to H.-M. Güther (Hoechst AG, Frankfurt am Main, Germany) for measurement of the thermal diffusivity.

References

1. Slack, G. A., Nonmetallic crystals with high thermal conductivity. *J. Phys. Chem. Solids*, **34** (1973) 321–35.
2. David, J. & Lang, J., Sur un nitrure double de magnésium et de silicium. *CR Acad. Sci. Paris*, **261** (1965) 1005–7.
3. David, J., Laurent, Y. & Lang, J., Structure de $MgSiN_2$ et $MgGeN_2$. *Bull. Soc. Fr. Mineral. Cristallogr.*, **93** (1970) 153–9.
4. Winterberger, M. Tcheou, F., David, J. & Lang, J., Verfeinerung der Struktur des Nitrids $MgSiN_2$—ein Neutronenbeugungsuntersuchung. *Z. Naturforsch.*, **35B** (1980) 604–6.
5. Wild, S., Grieveson, P. & Jack, K. H., The crystal chemistry of new metal-silicon-nitrogen ceramic phases. *Spec. Ceram.*, **5** (1972) 289–97.
6. Harris, R. K., Leach, M. J. & Thompson, D. P., Nitrogen-15 and oxygen-17 spectroscopy of silicates and nitrogen ceramics. *Chem. Mater.*, **4** (1992) 260–7.
7. Gaido, G. K., Dubrovskii, G. P. & Zykov, A. M., Photoluminescence of $MgSiN_2$ activated by europeum. *Izv. Akad. Nauk. SSSR, Neorg. Mater.*, **10** (1974) 564–6.
8. Pollard, H. F., *Sound Waves in Solids*. Pion Press, Amsterdam, The Netherlands, 1977.
9. Brown, W. F. & Srawley, J. E., *ASTM-STP-410*. ASTM, Philadelphia, PA, USA, 1966.
10. de With, G. & Hattu, N., On the use of small specimens in measurement of the fracture toughness for brittle materials. *J. Mater. Sci.*, **16** (1981) 1702–4.
11. Söllter, W. & Güther, H.-M., *Produktion und Prüftechnik*, **11** (1991) 106–9.
12. Joint Committee on Powder Diffraction Standards (JCPDS) card no. 25-530. JCPDS, Pennsylvania, USA.
13. Joint Committee on Powder Diffraction Standards (JCPDS) card no. 4-829. JCPDS, Pennsylvania, USA.
14. Joint Committee on Powder Diffraction Standards (JCPDS) card no. 9-250. JCPDS, Pennsylvania, USA.

15. Zykov, A. M., PhD thesis, Leningrad, USSR, 1975.
16. Joint Committee on Powder Diffraction Standards (JCPDS) card no. 34-189. JCPDS, Pennsylvania, USA.
17. Joint Committee on Powder Diffraction Standards (JCPDS) card no. 33-1160. JCPDS, Pennsylvania, USA.
18. Barin, L., Knacke, O. & Kubaschewski, O., *Thermochemical Properties of Inorganic Substances*. Springer Verlag, Berlin, Germany, 1977.
19. Morrell, R., *Handbook of Properties of Technical & Engineering Ceramics* (Part 2, Data Reviews). Her Majesty's Stationary Office, London, UK, 1987, 37–57.
20. Willems, H. X., van Hal, P. F., de With, G. & Metselaar, R., Mechanical and optical behaviour of gamma-aluminium oxynitride. *J. Mater. Sci.* (submitted). (See also Willems, H. X., Preparation and properties of translucent gamma-aluminium oxynitride. PhD thesis, Eindhoven University of Technology, The Netherlands, 1992.)
21. Landolt, H. & Börnstein, R., *Numerical Data and Functional Relationships in Science and Technology* (New Series). Springer, Berlin, Germany, 1980.
22. de With, G. & Hattu, N., High temperature fracture of hot-pressed AlN ceramics. *J. Mater. Sci.*, **18** (1983) 503–7.
23. Boch, P., Glandus, J. C., Jarrige, J., Lecompte, J. P. & Mexmain, J., Sintering, oxidation and mechanical properties of hot pressed aluminium nitride. *Ceram. Int.*, **8** (1982) 34–40.
24. Collins, A. T., Lightowlers, E. C. & Dead, P. J., Lattice vibration spectra of aluminum nitride. *Phys. Rev.*, **158** (1967) 833–8.
25. Grieg, J. W., System $MgO–SiO_2$. *Am. J. Sci.*, **37** (1927) 133–54.
26. Slack, G. A., Tanzill, R. A., Pohl, P. O. & Vandersande, J. W., The intrinsic thermal conductivity of AlN. *J. Phys. Chem. Solids*, **48** (1987) 641–7.
27. Harris, J. H., Youngman, R. A. & Teller, R. G., On the nature of the oxygen-related defect in aluminum nitride. *J. Mater. Res.*, **5** (1990) 1763–73.
28. Köstler, C., Güther, H.-M., Bestgen, H., Roosen, A. & Böcker, W., Influence of the microstructure on the thermal conductivity of AlN ceramics. *Proc. 2nd Eur. Conf. Adv. Mater. Processes*, Vol. 3. Institute of Materials, London, 1991, pp. 29–41.
29. Kröger, F. A. & Vink, J. H., Relations between the concentrations of imperfections in crystalline solids. *Solid State Physics*, **3** (1956) 307–435.
30. Touloukian, Y. S., Kirby, R. K. & Taylor, R. E. (ed.), *Thermophysical Properties of Matter*. Plenum, New York, USA, 1977.